JCTC Journal of Chemical Theory and Computation

Use of Block Hessians for the Optimization of Molecular Geometries

Jingzhi Pu and Donald G. Truhlar*

Department of Chemistry and Supercomputing Institute, 207 Pleasant Street S.E., Minneapolis, Minnesota 55455-0431

Received June 15, 2004

Abstract: We test a strategy for using block Hessians for transition state geometry optimizations. The block Hessian matrix is constructed by mixing a small critical block of the accurate Hessian for key atoms involved in bond breaking and forming with large noncritical blocks of the low-level Hessian. The method is tested for transition state optimizations at the MC-QCISD/3 level for five reactive systems: $H + CH_3OH$, $O + CH_4$, $OH + CH_4$, $NH_2 + CH_4$, and $H + C_2H_5OH$. When the entire low-level Hessian was used, significant oscillations were observed during the optimizations for the first four systems, whereas the transition state for the last system was optimized to a wrong structure. The block Hessian strategy efficiently removed these pathological effects of using low-level Hessians, and therefore it provides a highly reliable method for optimizing transition state structures with reduced computational cost. The method is very general, and it is especially well suited for optimizing transition state structures and equilibrium structures of large systems at very high levels of theory.

Use of molecular mechanics or electronic structure calculations to optimize molecular geometries or electronic structure calculations to optimize saddle points is one of the most common and important computational steps in modern theoretical chemistry.[1] The foundation algorithm for geometry optimization is the iterative Newton−Raphson algorithm;[2] however, most optimizations are carried out with simplified versions of this algorithm, which are often called quasi-Newton methods. A serious impediment to using full Newton−Raphson calculations is that they require a Hessian at every iteration, and Hessians are expensive, especially for the more reliable levels of electronic structure theory. Furthermore, as system size increases the number of Hessian elements increases as the square of the number (N) of atoms.

There are two main strategies in use to decrease the cost of Hessian evaluations in geometry optimization. We assume that one wants the geometry optimized at electronic structure level L. One strategy would be to use approximate Hessians at level L. For example, at a previous iteration one might have computed an accurate level-L Hessian at geometry $\mathbf{R}$. Now the iterations have advanced the geometry to $\mathbf{R}'$. One can use gradient calculations at recent iterations to approximately update the Hessian to $\mathbf{R}'$. A variation on this first strategy is to use the accurate Hessian at $\mathbf{R}$ (without updates) as an approximate Hessian at $\mathbf{R}'$. The second strategy is to use accurate Hessians at a lower level L'. For example one might use Hartree−Fock (HF) Hessians[3] to optimize a geometry at the higher level of quadratic configuration interaction with single and double excitation[4] (QCISD).

$$\begin{pmatrix} \text{CC} & \text{CN} \\ \text{NC} & \text{NN} \end{pmatrix}$$

Figure 1. The coordinates are divided into a critical (C) group and a noncritical (N) group and the Hessian matrix is blocked accordingly.

The purpose of this article is to consider a third general strategy for minimizing the Hessian cost and to demonstrate that it can be used successfully. The strategy consists of blocking the Hessian matrix, as in Figure 1, and treating the critical block or blocks at a high level and less critical blocks at a lower level. For example, consider the reaction

$$OH + C_nH_{2n+2} \rightarrow H_2O + C_nH_{2n+1} \qquad \text{(R1)}$$

If we label the acceptor oxygen atom, the transferred

10.1021/ct0400020 CCC: $30.25
Published on Web 11/02/2004

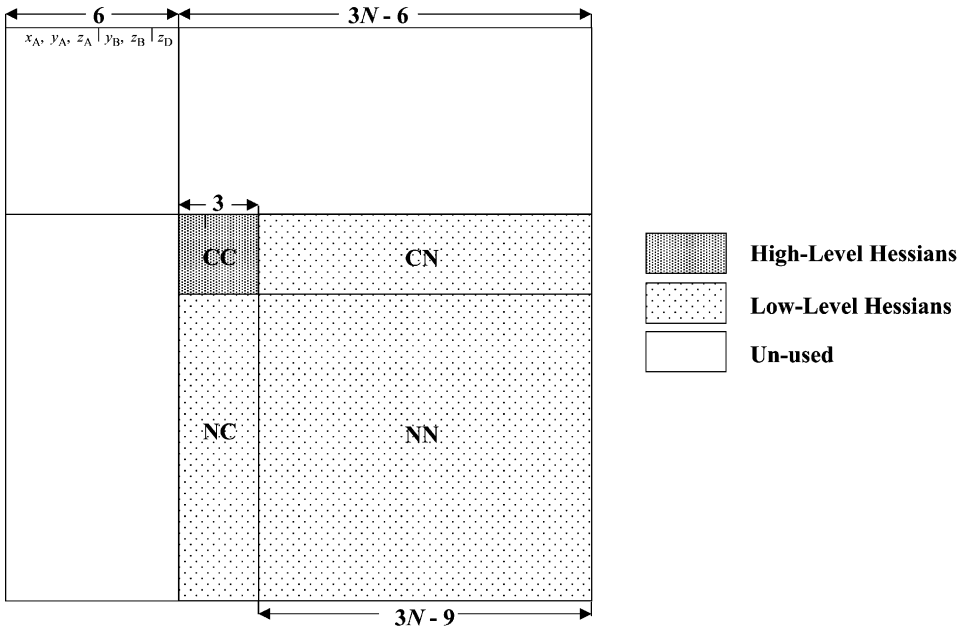

Figure 2. Another partition of the Hessian matrix where the size of the critical block is reduced from 9 × 9 to 3 × 3.

hydrogen atom, and the donor carbon atom as critical (C) and all other atoms as noncritical (N), the number of elements of the CC block is 81, the number of elements of CN and NC blocks is $162n + 54$, and the number of elements of the NN block is $81n^2 + 54n + 9$. Thus if we need high-level Hessians only for the blocks involving critical atoms (CC, CN, and NC), we will have changed the quadratic scaling to linear scaling. Already at $n = 8$, the number of Hessian elements to be evaluated at the high level is reduced by a factor of 5. Furthermore, if we only need the high-level Hessian for the CC block, the number of high-level Hessian elements required is a constant irrespective of the system size n. Thus if this strategy works (and the present paper show that it does), one should be able to optimize much larger structures at high (expensive) levels of electronic structure theory. Thus this approach has the potential to revolutionize computational strategies for electronic structure calculations on large systems.

The strategy tested here is expected to be especially useful for optimizations at very high levels where the Hessians are usually evaluated by numerical differentiation of very expensive gradients or energies. In such cases it is easy to carry out numerical differentiation of any desired subset of Hessians. For large systems one could imagine using sophisticated labeling and blocking schemes to identify the critical subset of Hessian elements. In this article, we will use the simple scheme of Figure 1 where the CC block consists of 3 Cartesian degrees of freedom for a donor atom, 3 for a transferred element, and 3 for an acceptor atom, and high-level Hessians are only calculated for this 9 × 9 critical block.

Having chosen a 9 × 9 critical block, we can, however, achieve a further efficiency by a strategic choice of the origin and the orientation of the molecule. When we use unblocked Hessians and optimize a geometry, we can place the first atom (A) at the origin ($x_A = y_A = z_A = 0$), the second atom (B) on the x axis ($y_B = z_B = 0$), and the third atom (D) to lie in the xy plane ($z_D = 0$). During the optimization these six coordinates are held fixed, and only $3N - 6$ coordinates vary. In the blocked method, we can always number the acceptor, donor, and transferred atom as the first three atoms. This partitions the 9 Cartesian coordinates of these atoms into 6 fixed critical coordinates and 3 nonfixed critical coordinates (these will be called the active coordinates). Since we do not need gradients or Hessian elements for the fixed atoms, this reduces the size of the CC block that needs to be calculated to 3 × 3. This new blocking is shown in Figure 2. To calculate the full $3N \times 3N$ Hessian at **R** by forward differentiation requires (in addition to a gradient at **R**) a total of $3N$ additional gradients, each one displaced in one of the coordinates. To calculate high-level Hessians for the 3 × 3 critical block requires only 3 gradients in addition to the one at **R**. In the implementation below, we calculate a new Hessian every third step. Thus, on average, the number of gradients required per step for calculating the Hessian is decreased from $3N + 1$ to 2.

Although the kind of strategy tested here has been mentioned as a possible approach in a pedagogical article,[5] and although the *Gaussian* program[6] allows numerical estimation of certain elements of the Hessian in internal coordinates, we know of no published examples of the kind of treatment espoused here. Furthermore the advantages of using this approach even with more straightforward and more general Cartesian optimization do not seem to be recognized by many current workers in the field. Therefore, in the

present article, we present several examples showing the power of the method.

In the first set of tests, the transition states for the following reactions are considered:

$$H + CH_3OH \rightarrow H_2 + CH_2OH \quad (R2)$$

$$O + CH_4 \rightarrow OH + CH_3 \quad (R3)$$

$$OH + CH_4 \rightarrow H_2O + CH_3 \quad (R4)$$

$$NH_2 + CH_4 \rightarrow NH_3 + CH_3 \quad (R5)$$

We carried out transition state geometry optimizations for the above four systems at the level of multicoefficient quadratic configuration interaction with single and double excitations, version 3 (MC-QCISD/3).[7,8] The MC-QCISD method belongs to the family of multicoefficient correlation methods (MCCMs),[7−11] which have been shown to be able to provide accurate atomization energies, reaction barrier heights, and transition state geometries at highly correlated levels. From a practical point of view, MC-QCISD represents the most accurate available method for which the computational effort[12] of energy calculations scales as N^6, where N is the number of atoms in the system. (Methods with steeper scaling are usually not affordable for studying medium- to large-sized systems.) However, the method used here is applicable to other levels[12] of electronic structure theory like MP2, MP4, QCISD, CCSD(T), etc. The MC-QCISD total energy and gradients are composed of a linear combination of several single-level components, i.e., HF/6-31G(d), HF/MG3S, MP2/6-31G(d), MP2/MG3S, and QCISD/6-31G(d).[7] The MG3S[13] basis set is identical to 6-311+G(2df,2p)[14] for systems containing only first row elements. In the current implementation[15] where single-level calculations are carried out using *Gaussian 98*,[6] the MC-QCISD analytical gradient is available; however, the MC-QCISD Hessian is obtained numerically due to the unavailability of an analytical Hessian for the QCISD component.

We will test the new idea by comparing the use of a high-level Hessian for a critical block to using the entire low-level Hessian. For this purpose we use a very straightforward optimization algorithm, in particular, the Newton−Raphson method[2] implemented in program MULTILEVEL.[15] To reduce the cost of calculating Hessians every Newton−Raphson step, we apply two different approaches.

In the first approach,[11] the Hessian matrix is calculated every three Newton−Raphson steps and is kept frozen until the next recalculated point. Whenever a Hessian recalculation is requested, either an entire low-level Hessian (LH) at level L or the blocked Hessian (BH, with the critical block at a high-level and the rest at a low level) is provided.

In the second approach, we test whether the block Hessian idea can be combined with Hessian update techniques to further improve the efficiency of the method. In particular, the LH or BH is only calculated at the first step and is updated for later steps during the geometry optimization. Because our strongest interest is transition structure searching, we use the Davidon-Fletcher-Powell (DFP) Hessian update scheme[16] which does not preserve a positive definite Hessian matrix. (Alternatively, one could use the improved Powell formula of Bofill,[17] which is probably the best update method for transition states.)

In the present article, the low-level L is taken as HF/6-31G(d) or AM1. The former choice has been shown to be good enough for carrying out multilevel optimizations for small stable species.[11]

The block Hessian matrix is obtained by forward differentiation of the analytical gradients for the Cartesian coordinates of critical atoms. (The use of forward differences saves a factor of 2 in computer time as compared to central differentiations.) For atom transfer reactions, such as the reactions tested in the present paper, by using the 9×9 critical block scheme described above, this algorithm involves 9 gradient calculations in total associated with 9 finite displacements of each Cartesian coordinate of the active atom

$$\frac{\partial^2 E}{\partial x_i \partial x_j} = \frac{g_{x_i}|_{x_j+\delta x} - g_{x_i}|_{x_j}}{\delta x} \quad (i, j = 1 - 9) \qquad (1)$$

where E is the total electronic energy of the system; x_i is ith Cartesian coordinate of a row or column of the critical block; g_{x_i} is the Cartesian gradient component corresponding to the coordinate x_i; and δx is a finite displacement. With the particular choice of geometry specified in the 3×3 critical block scheme, the blocked method only requires 3 gradient calculations to evaluate the high-level Hessian elements for the 3 active coordinates. In the tests presented below, we will apply the new method to a 9×9 critical block scheme and then repeat some of the calculations with the 3×3 critical block scheme.

It is worthwhile to point out that the CN and NC blocks of the Hessian matrix are also available by above numerical differentiations of the analytical gradients. However, we restrict the usage of high-level Hessian elements only to the CC block throughout the present study. This strategy is especially appealing for cases where analytical gradients are also very expensive or even analytically unavailable; in the latter case one could use a second order numerical differentiation of the energies to obtain a fairly small critical block of the accurate Hessian without calculating other gradient components to as high a precision.

The initial geometries used in the optimizations were obtained from three different levels of theory, i.e., HF/6-31G(d), B3LYP/6-31G(d), and QCISD/MG3. The optimization is considered to be complete if the maximum component of the gradient is less than 10^{-4} hartree/bohr. Table 1 lists key distances for bond breaking and forming in these initial geometries compared to the fully optimized geometries at the MC-QCISD/3 level.

We tabulate the energies and maximum gradients during the optimization process for transition states of R2 and R3 in Tables 2 and 3. It is observed a large number of cases in investigation hardly converged if the entire low-level Hessian is used. The case starting with the HF/6-31G(d) geometry is quickly converged using low-level Hessians; however, this may be fortuitous. For converged cases, Tables 2 and 3 estimate the cost in terms of the number of gradient calculations for the optimization. Among the six cases in

Table 1. Breaking and Forming Bond Distances in Initial Geometries Compared to Those in MC-QCISD/3 Optimized Geometries for Reactions R2−R6

	I[a]	II[b]	III[c]	IV[d]
R2				
C−H	1.351	1.302	1.316	1.307
H−H	0.959	1.011	0.969	0.976
R3				
C−H	1.369	1.389	1.302	1.275
H−O	1.167	1.147	1.202	1.226
R4				
C−H	1.313	1.274	1.227	1.194
H−O	1.200	1.238	1.285	1.320
R5				
C−H	1.358	1.355	1.314	1.298
H−N	1.252	1.248	1.270	1.287
R6				
C−H	1.340	1.268	nc[e]	1.282
H−H	0.969	1.054	nc[e]	1.000

[a] HF/6-31G(d) geometry. [b] B3LYP/6-31G(d) geometry. [c] QCISD/MG3 geometry. [d] Optimized geometry at the MC-QCISD/3 level. [e] nc denotes not calculated.

Tables 2 and 3, five of them display oscillations if the entire low-level Hessian (LH) is used, but using the block Hessian (BH) removes these oscillations in all cases. Although the high-level Hessian (HH) works equally as well as the BH, the cost of computing all the elements numerically makes it unfeasible for systems of large size, which prevents applying this approach to many interesting problems.

To evaluate the new BH method more systematically, we apply a statistical approach. Combining three different initial geometries, two levels of the low-level Hessian, and two Hessian update schemes for reactions R2−R5, we have 48 cases in total. The numbers of converged cases have been collected based on various conditions in Table 4, for both the LH and the BH methods. The notation X/Y represents that there are X cases successfully converged among Y cases that satisfy the conditions described in the first column of Table 4. If the entire low-level Hessian is used, only 11 of the 48 cases converge within 30 iterations. It is encouraging that the number of converged cases is significantly increased to 29 when the block Hessian strategy is applied, which is almost three times more robust compared to the method that simply uses the low-level Hessian. Table 4 indicates that the BH strategy outperforms the LH one over broad range of reactions, initial geometries, levels of theory to calculate the Hessian, and Hessian update schemes. In Table 5, we collected the statistics for R2 and R3 with the 3×3 critical block version of the BH strategy (as shown in Figure 2). Using the 3×3 critical block further improves the efficiency of the BH geometry optimization, and the stability of the algorithm is not altered.

The above tests show that the quality of the critical block of the Hessian matrix plays an important role in geometry optimizations of transition state structures. The errors of using low-level Hessian to approximate the high-level Hessian sometimes can be so significant that the optimizations oscillate wildly even if one starts from a geometry close to the high-level saddle point, for example, the QCISD/MG3 geometry (see comparisons of key bond distances in Table 1). The oscillations of energies during the optimization are not the only pathological behavior when the low-level Hessian is used; the transition state can also be optimized to

Table 2. Maximum Component of the Gradient (in au) for Transition State Optimization of $H + CH_3OH \rightarrow H_2 + CH_2OH$ at the MC-QCISD/3 Level Using Low-Level Hessians (LH), Block Hessians (BH, as Figure 1), and High-Level Hessians (HH)

	I[a]			II[b]			III[c]		
iteration	LH[d]	BH[e]	HH[f]	LH	BH	HH	LH	BH	HH
0	1.6E−2	1.6E−2	1.6E−2	9.2E−3	9.1E−3	9.1E−3	5.0E−3	5.0E−3	5.0E−3
1	2.6E−3	2.9E−3	1.0E−2	3.5E−3	1.9E−3	4.0E−4	7.0E−4	6.2E−4	2.2E−4
2	9.9E−4	1.5E−3	3.5E−2	4.3E−3	8.1E−4	1.3E−4	3.0E−4	2.7E−4	2.0E−4
3	2.1E−3	8.0E−4	6.0E−2	1.8E−3	4.2E−4	7.1E−5	1.6E−3	1.2E−4	6.2E−4
4	2.4E−4	3.8E−4	9.8E−2	1.2E−2	2.7E−4		4.8E−3	5.7E−5	2.4E−4
5	1.4E−4	2.8E−4	6.9E−2	1.0E−2	1.9E−4		1.2E−3		5.4E−5
6	5.8E−5	2.5E−4	8.8E−2	9.8E−3	1.4E−4		5.1E−3		
7		2.2E−4	4.8E−2	1.2E−2	1.1E−4		6.8E−3		
8		1.9E−4	7.2E−2	5.0E−3	9.2E−5		5.3E−3		
9		1.7E−4	1.0E−1	1.7E−2			2.6E−3		
10		1.5E−4	5.9E−2	1.5E−2			2.0E−3		
11		1.4E−4	8.4E−2	7.1E−3			1.1E−3		
12		1.2E−4	1.0E−1	2.2E−2			3.0E−3		
13		1.1E−4	6.4E−2	2.4E−2			1.1E−2		
14		9.8E−5	2.6E−2	6.9E−3			9.5E−4		
15			4.0E−2	3.3E−2			8.0E−3		
16			3.2E−2	3.6E−3			9.1E−3		
17			4.0E−3	6.2E−2			7.3E−3		
18			2.1E−3	8.1E−2			6.5E−3		
cost[g]	7	60	nc[h]	nc[h]	36	46	nc[h]	23	90

[a] HF/6-31G(d) initial geometry. [b] B3LYP/6-31G(d) initial geometry. [c] QCISD/MG3 initial geometry. [d] For the LH column, the HF/6-31G(d) level is used for the entire Hessian, and a new Hessian is computed at every third iteration; no Hessian update schemes are used. [e] Use the 9×9 critical block scheme. [f] Central differentiations of gradients are used. [g] In terms of gradient calculations. [h] nc denotes not converged within 30 iterations.

Table 3. Maximal Gradient for Transition State Optimization of $O + CH_4 \rightarrow OH + CH_3$ at the MC-QCISD/3 Level Using Low-Level Hessians (LH), Block Hessians (BH, as Figure 1), and High-Level Hessians (HH)

	I[a]			II[b]			III[c]		
iteration	LH[d]	BH[e]	HH[f]	LH	BH	HH	LH	BH	HH
0	1.5E−2	1.5E−2	1.5E−2	1.8E−2	1.8E−2	1.8E−2	5.7E−3	5.7E−3	5.7E−3
1	9.8E−3	6.4E−3	4.4E−2	1.3E−2	6.7E−3	9.3E−3	3.6E−3	2.6E−3	5.2E−4
2	7.5E−3	2.5E−3	2.4E−3	7.7E−3	3.0E−3	6.1E−3	2.2E−3	1.1E−3	9.2E−5
3	4.4E−2	1.3E−3	1.5E−3	4.4E−3	1.8E−3	6.2E−3	1.3E−3	4.6E−4	
4	7.4E−3	5.9E−4	4.0E−4	2.6E−3	8.6E−4	7.5E−4	7.2E−4	2.1E−4	
5	2.8E−2	2.7E−4	8.5E−4	1.5E−3	4.1E−4	4.0E−5	6.4E−4	9.3E−5	
6	5.8E−2	1.3E−4	3.3E−3	8.4E−4	1.9E−4		1.3E−3		
7	3.5E−2	5.9E−5	1.4E−4	6.3E−4	9.6E−5		1.4E−3		
8	6.3E−2		2.4E−5	1.1E−3			2.6E−3		
9	1.3E−1			2.0E−3			5.0E−3		
10	1.0E−1			2.0E−3			4.8E−3		
11	5.2E−2			3.8E−3			1.1E−2		
12	9.5E−2			7.6E−3			2.0E−2		
13	8.2E−2			7.5E−3			1.6E−2		
14	7.4E−2			1.4E−2			4.3E−2		
15	4.8E−2			2.8E−2			7.0E−2		
16	6.2E−2			2.6E−2			6.7E−2		
17	7.0E−2			5.7E−2			1.7E−1		
18	9.3E−2			7.6E−2			7.3E−2		
cost[g]	nc[h]	35	117	nc[h]	35	78	nc[h]	24	39

[a] HF/6-31G(d) initial geometry [b] B3LYP/6-31G(d) initial geometry [c] QCISD/MG3 initial geometry [d] For the LH column, the HF/6-31G(d) level is used for the entire Hessian, and a new Hessian is computed at every third iteration; no Hessian update schemes are used. [e] Use the 9×9 critical block scheme. [f] Central differentiations of gradients are used. [g] In terms of gradient calculations. [h] nc denotes not converged within 30 iterations.

Table 4. Statistics of the Convergence Cases Using the Entire Low-Level Hessian (LH) and the Block Hessian (BH) Strategy (as Figure 1)

collect by	LH	BH[a]
reaction		
R2	4/12	7/12
R3	1/12	9/12
R4	3/12	7/12
R5	3/12	6/12
initial geometry		
HF/6-31G(d)	3/16	8/16
B3LYP/6-31G(d)	2/16	9/16
QCISD/MG3	6/16	12/16
low-level Hessian		
HF/6-31G(d)	8/24	16/24
AM1	3/24	13/24
Hessian update scheme		
no update[b]	5/24	18/24
DFP	6/24	11/24
in total		
	11/48	29/48

[a] This table is based on the 9×9 scheme for the high-level block. [b] LH or BH Hessians are calculated every three steps and kept frozen until the next recalculation point.

Table 5. Statistics of the Convergence Cases Using the Entire Low-Level Hessian (LH) and the Block Hessian (BH) Strategy (as Figure 2)

collect by	LH	BH[a]
reaction		
R2	2/12	7/12
R3	6/12	10/12
initial geometry		
HF/6-31G(d)	2/8	4/8
B3LYP/6-31G(d)	3/8	6/8
QCISD/MG3	3/8	7/8
low-level Hessian		
HF/6-31G(d)	2/12	9/12
AM1	6/12	8/12
Hessian update scheme		
no update[b]	5/12	9/12
DFP	3/12	8/12
in total		
	8/24	17/24

[a] This table is based on the 3×3 scheme for the high-level block. [b] LH or BH Hessians are calculated every three steps and kept frozen until the next recalculation point.

a wrong structure. One of the examples of this type is the transition state optimization for the following reaction:

$$H + C_2H_5OH \rightarrow H_2 + C_2H_4OH \qquad \text{(R6)}$$

In Figures 3 and 4, we plot the energies as function of the optimization step for cases in which HF/6-31G(d) and B3LYP/6-31G(d) geometries were used as an initial geometry. Both Figures 3 and 4 show that using the low-level Hessian can result in a low-energy structure other than the true saddle point (it is a reactant-like structure), but using the block Hessian corrects this error straightforwardly and makes the optimizations much more stable.

The emphasis in the present article has been on saddle point optimization at high levels of electronic structure theory in medium-size molecules. When analytic Hessians are not available, computing the numerical Hessian presents a computational bottleneck for geometry optimizations if the

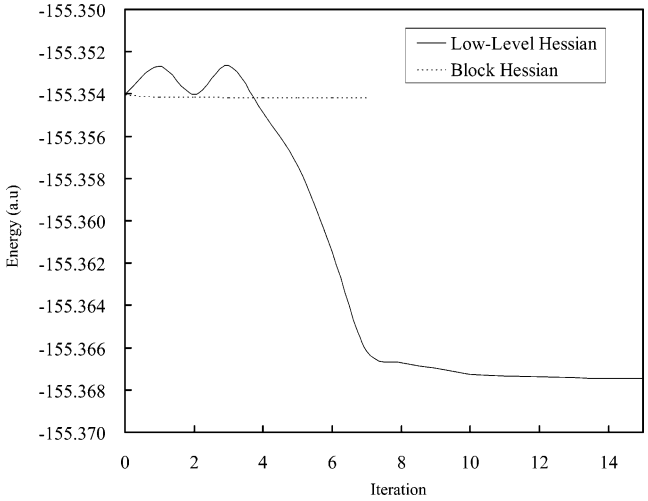

Figure 3. Energy of the transition state optimization for H + $C_2H_5OH \rightarrow H_2 + C_2H_4OH$ using the low-level Hessian at HF/6-31G(d) level or block Hessians. For the block Hessian optimization, the 9 × 9 scheme for the high-level block is used. The HF/6-31G(d) geometry is used as the initial geometry.

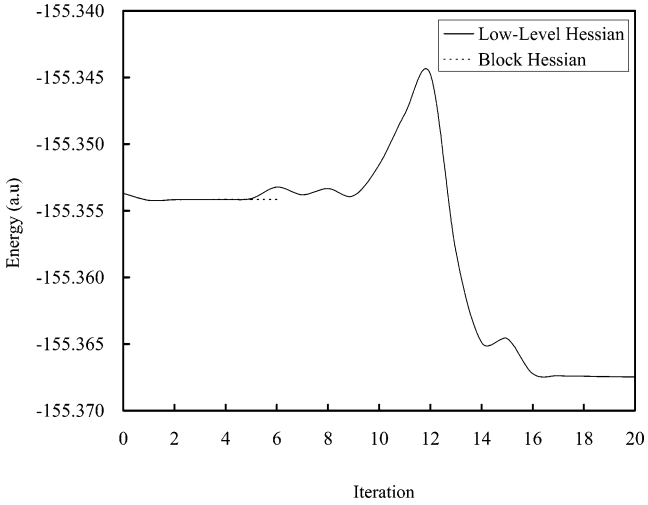

Figure 4. Energy of the transition state optimization for H + $C_2H_5OH \rightarrow H_2 + C_2H_4OH$ using the low-level Hessian at HF/6-31G(d) level or block Hessians. For the block Hessian optimization, the 9 × 9 scheme for the high-level block is used. The B3LYP/6-31G(d) geometry is used as the initial geometry.

optimization algorithm requires full Hessians. In such a case the cost is dominated by the calculations of the Hessians, at least when the present blocked Hessian method is not used. As we mentioned above, one may use the lower-level Hessian as an alternative to approximate the true Hessian during the optimization procedure. Because a low-level Hessian, especially if computed analytically and by a method with lower scaling order than the high-level Hessian, is relatively computationally inexpensive, one may hope that it provides a satisfactory solution that alleviates the bottleneck of computing numerical high-level Hessian during geometry optimizations. However, for some difficult cases, especially for transition state geometry optimizations, using a low-level Hessian is not powerful enough because the transition vector (the eigenvector associated with a negative eigenvalue) to bring the system to a first-order saddle point is very sensitive to the accuracy of the Hessian.[17] For this kind of situation, the accurate description of the key Hessian elements involved in the bond breaking and forming is crucial to direct the optimization to the correct transition state structure, and the present method may be especially useful.

Another case of interest is for very large molecules with lower levels of electronic structure theory (for example, neglect-of-diatomic-differential-overlap molecular orbital theory) where the cost is dominated not by the calculation of the Hessian but by its diagonalization. A scheme that splits the system into a reaction core and its environment has also been found to be useful in that case.[18]

The present paper has used an algorithm in Cartesian coordinates, although there are some well-known advantages to optimizing in internal coordinates. The advantages of Cartisian coordinates are also well-known,[19] namely the simplicity and generality of the algorithms used and the automatic avoidance of redundancies. In contrast, the advantage of internal coordinates is that when they are chosen physically, for example, as valence internal coordinates (bond stretches, valence angle bends, and torsions), they eliminate much of the coupling between Cartesians. Our experience, however, and that of others[19,20] is that optimization in Cartesian coordinates can be very efficient when Hessian information is used. Furthermore, Cartesians are much preferred to internal coordinates for solid-state optimizations[21] or surface science,[22] where internals can be very cumbersome, or for clusters.[20] A key result of this paper is that Cartesians can remain efficient even when only a small portion of the Hessian is computed at the high electronic structure level at which saddle point optimization is required. As mentioned above, partial Hessians can also be used with internal coordinates.

There is considerable interest in combined quantum mechanical and molecular mechanical methods for electronic structure calculations, and this is a special case of the need for multiscale[23] and multilevel[24,25] algorithms. To treat large systems efficiently, one requires such algorithms not only for the electronic structure step but also for other steps such as geometry optimizations, computational thermochemistry, and dynamics. The present article presents such a scheme suitable for geometry optimization.

References

(1) Schlegel, H. B. *Adv. Chem. Phys.* **1987**, *67*, 249.

(2) Press, W. H.; Teukolsky, S. A.; Vetterling, W. T.; Flannery, B. T. *Numerical Recipes*, 2nd ed.; Cambridge University Press: Cambridge, 1992; pp 372 ff.

(3) Pople, J. A.; Krishnan, R.; Schlegel, H. B.; Binkey, J. S. *Int. J. Quantum Chem. Symp.* **1979**, *13*, 225.

(4) Pople, J. A.; Head-Gorden, M.; Raghavachari, K. *J. Chem. Phys.* **1987**, *87*, 5968.

(5) Schlegel, H. B. In *New Theoretical Concepts for Understanding Organic Reactions*; Bertrán, J. Csizmadia, I. G., Eds.; NATO ASI Series C 267; Kluwer: Dordrecht, 1989; p 33. See p 48.

(6) *Gaussian98*, by M. J. Frisch, G. W. Trucks, H. B. Schlegel, G. E. Scuseria, M. A. Robb, J. R. Cheeseman, V. G. Zakrzewski, J. A. Montgomery, R. E. Stratmann, J. C.

Burant, S. Dapprich, J. M. Millam, A. D. Daniels, K. N. Kudin, M. C. Strain, O. Farkas, J. Tomasi, V. Barone, M. Cossi, R. Cammi, B. Mennucci, C. Pomelli, C. Adamo, S. Clifford, J. Ochterski, G. A. Petersson, P. Y. Ayala, Q. Cui, K. Morokuma, D. K. Malick, A. D. Rabuck, K. Raghavachari, J. B. Foresman, J. Cioslowski, J. V. Ortiz, B. B Stefanov, G. Liu, A. Liashenko, P. Piskorz, I. Komaromi, R. Gomperts, R. L. Martin, D. J. Fox, T. Keith, M. A. Al-Laham, C. Y. Peng, A. Nanayakkara, C. Gonzalez, M. Challacombe, P. M. W. Gill, B. G. Johnson, W. Chen, M. W. Wong, J. L. Andres, M. Head-Gordon, E. S. Replogle, and J. A. Pople, Gaussian, Inc., Pittsburgh, PA, 1998.

(7) Lynch, B. J.; Truhlar, D. G. *J. Phys. Chem. A* **2003**, *107*, 3898.

(8) Fast, P. L.; Truhlar, D. G. *J. Phys. Chem. A.* **2000**, *104*, 6111.

(9) Tratz, C. M.; Fast, P. L.; Truhlar, D. G. *PhysChemComm* **1999**, *2*, Article 14.

(10) Fast, P. L.; Sanchez, M. L.; Truhlar, D. G. *Chem. Phys. Lett.* **1999**, *306*, 407.

(11) Rodgers, J. M.; Fast, P. L.; Truhlar, D. G. *J. Chem. Phys*. **2000**, *112*, 3141.

(12) Raghavachari, K.; Anderson, J. B. *J. Phys. Chem*. **1996**, *100*, 12960.

(13) Lynch, B. J.; Zhao, Y.; Truhlar, D. G. *J. Phys. Chem. A* **2003**, *107*, 1384.

(14) Krishnan, R.; Binkley, J. S.; Seeger, R.; Pople, J. A. *J. Chem. Phys.* **1980**, *72*, 650.

(15) Rodgers, J. M.; Lynch, B. J.; Fast, P. L.; Zhao, Y.; Pu, J.; Chuang, Y.-Y.; Truhlar, D. G. MULTILEVEL-version 3.1; University of Minnesota, Minneapolis, 2003.

(16) Press, W. H.; Teukolsky, S. A.; Vetterling, W. T.; Flannery, B. P. *Numerical Recipes in Fortran 77*; Cambridge University Press: Cambridge, 1992; pp 418 ff.

(17) Bofill, J. M. *Intern. J. Quantum Chem*. **2003**, *94*, 324.

(18) Turner, A. J.; Moliner, V.; Williams, I. H. *Phys. Chem. Chem. Phys*. **1999**, *1*, 1323.

(19) Baker, J.; Hehre, W. J. *J. Comput. Chem*. **1991**, *12*, 606. Baker, J. *J. Comput. Chem*. **1993**, *14*, 1085.

(20) Niesse, J. A.; Mayne, H. R. *J. Chem. Phys*. **105**, *4700*, 1996.

(21) Ke, X.; Tanaka, I. *Phys. Rev. B* **2004**, *69*, 165114/1.

(22) Ciobica, I. M.; Frechard, F.; van Santen, R. A.; Kleyn, A. W.; Hafner, J. *J. Phys. Chem. B* **2000**, *104*, 3364.

(23) Butalov, V. V.; Rubia, T. D. d. l.; Phillips, P.; Kaxiras, E.; Ghoniem, N. *Multiscale Modeling of Materials*; Materials Research Society: Pittsburgh, 1999.

(24) Corchado, J. C.; Truhlar, D. G. *ACS Symp. Ser*. **1998**, *712*, 106.

(25) Petersson, G. A. *ACS Symp. Ser*. **1998**, *677*, 237.

CT0400020